J. Great Lakes Res. 30(1):148–165
Internat. Assoc. Great Lakes Res., 2004

Wind Fields over the Great Lakes Measured by the SeaWinds Scatterometer on the QuikSCAT Satellite

Son V. Nghiem[1,*], George A. Leshkevich[2], and Bryan W. Stiles[1]

[1]*Jet Propulsion Laboratory*
California Institute of Technology
4800 Oak Grove Drive, MS 300-235
Pasadena, California 91107

[2]*National Oceanic and Atmospheric Administration*
Great Lakes Environmental Research Laboratory
2205 Commonwealth Blvd.
Ann Arbor, Michigan 48105

ABSTRACT. *This paper demonstrates the utility of satellite scatterometer measurements for wind retrieval over the Great Lakes on a daily basis. We use data acquired by the SeaWinds Scatterometer on the QuikSCAT (QSCAT) satellite launched in June 1999 to derive wind speeds and directions over the lakes at a resolution of 12.5 km, which is two times finer than the QSCAT standard ocean wind product at a resolution of 25 km. To evaluate QSCAT performance for high-resolution measurements of lake wind vectors, we compare QSCAT results with Great Lakes Coastal Forecasting System (GLCFS) nowcast wind fields and with standard QSCAT measurements of ocean wind vectors. Although the satellite results over the Great Lakes are obtained with an ocean model function, QSCAT and GLCFS wind fields compare well together for low to moderate wind conditions (4–32 knots). For wind speed, the analysis shows a correlation coefficient of 0.71, a bias of 2.6 knots in mean wind speed difference (nowcast wind is lower) with a root-mean-square (rms) deviation of 3.8 knots. For wind direction, the correlation coefficient is 0.94 with a very small value of 1.3° in mean wind direction bias and an rms deviation of 38° for all wind conditions. When excluding the low wind range of 4–12 knots, the rms deviation in wind direction reduces to 22°. Considering QSCAT requirements designed for ocean wind measurements and actual evaluations of QSCAT performance over ocean, results for high-resolution lake wind vectors indicate that QSCAT performs well over the Great Lakes. Moreover, we show that wind fields derived from satellite scatterometer data before, during, and after a large storm in October 1999, with winds stronger than 50 knots, can monitor the storm development over large scales. The satellite results for storm monitoring are consistent with GLCFS nowcast winds and lake buoy measurements. A geophysical model function can be developed specifically for the Great Lakes using long-term data from satellite scatterometers, to derive more accurate wind fields for operational applications as well as scientific studies.*

INDEX WORDS: *Great Lakes, wind fields, storm, remote sensing, satellite, scatterometer.*

INTRODUCTION

The objective of this study is to investigate the utility of satellite scatterometry for Great Lakes wind field mapping with large spatial coverage and high temporal resolution. The SeaWinds Scatterometer on the QuikSCAT Satellite has acquired data continuously over the Great Lakes since July 1999, and future satellite scatterometers can extend the dataset for long-term wind measurements.

Monitoring wind fields on a regional scale over the Great Lakes is useful for marine resource management, lake fisheries and ecosystem studies, navigation hazard forecast, and as input data or verification of interpolated and gridded wind fields for hydrodynamic circulation and wave prediction models. Storms with strong winds and high waves over the Great Lakes can cause extensive flooding, severe erosion, property damage, and loss of lives

*Corresponding author. E-mail: Son.V.Nghiem@jpl.nasa.gov

across vast regions (Gabriel *et al*. 1997, Lawrence 1995, Angel 1995, Khandekar and Swail 1995, Shabica and Pranschke 1994, Kreutzwiser and Gabriel 1992, Martner *et al*. 1992). The Great Lakes have strong effects on passing cyclones and can accelerate and intensify the cyclones (Davidson-Arnott and Fisher 1992) producing storm-force winds with heavy precipitation (Miner *et al*. 2000). Storm surges impact wetlands, tributaries, and estuaries (Bedford 1992) and episodic wind events, causing resuspension and transport of sediments and associated constituents, can exert major influences on ecosystems (Eadie *et al*. 2002 and 1996). A small summer storm or wind event can disrupt the development of several zooplankton populations in the Great Lakes ecosystem (Krieger and Klarer 1991) or contribute to the development of a plankton bloom (Lesht *et al.* 2002). According to Schwab (1989), perhaps the most important input in successful wave and storm surge hindcasting and forecasting is an accurate specification of the wind field. Furthermore, "not only does the accuracy of the forecast wind field limit the accuracy of the wave or storm surge forecast, but when inaccurate hindcast wind fields are used for model calibration and development, serious errors may become built into the model and permanently degrade the accuracy of the model" (Schwab 1989).

While numerous surface stations measure winds on land along the lakeshore and buoys measure winds at several lake locations during ice-free months, to date there is no systematic measurement of high-resolution wind fields over all the lakes on a daily basis. Synthetic Aperture Radar (SAR) data have been used to derive very high-resolution winds (Fetterer *et al*. 1998, Horstmann *et al*. 2000, Monaldo *et al.* 2001). However, the SAR inversion of wind fields for both speed and direction has an inherent problem of underdetermination (Portabella *et al.* 2002) and end-to-end calibration of multi-beam SARs is difficult and largely undemonstrated (Beal 2000). Due to a limited swath width (e.g., 500 km for RADARSAT ScanSAR Wide A mode), a SAR may cover a part of the Great Lakes in one day and another part on a different day, and a daily coverage of the entire Great Lakes (all five large lakes) is not possible with any current satellite SAR. Most importantly, no consistent and continuous time-series of SAR data have ever been ordered nor collected to derive Great Lakes winds even on a monthly basis let alone a weekly or daily basis, and no operational U.S. satellite SAR mission has been planned for wind measurements.

In this paper, we demonstrate the use of satellite scatterometry to monitor daily wind fields over all Great Lakes. From satellite scatterometer data, we derive surface wind vectors over the lakes as a special product with a resolution of 12.5 km compared to the standard wind retrieval product at 25-km resolution. With the higher resolution, the special wind field grid is sufficient to represent the wind field over the Great Lakes. We verify the satellite results from low wind to gale and storm-force conditions with buoy data and with model nowcast wind results from the Great Lakes Coastal Forecasting System (GLCFS) run at the National Oceanic and Atmospheric Administration (NOAA) Great Lakes Environmental Research Laboratory (GLERL). This is the first paper that presents such high-resolution wind fields derived from satellite radar (either SAR or scatterometer) data over the Great Lakes (freshwater surface), as all previously published work is for the ocean surface (saline seawater). As benchmarks, we provide references on various comparisons of ocean wind results to assess the current performance of the scatterometer for high-resolution measurements of Great Lakes wind fields. Then, we discuss possible future improvements.

SCATTEROMETER MEASUREMENTS OF WIND VECTOR

SeaWinds Scatterometer on QuikSCAT Satellite

The National Aeronautics and Space Administration (NASA) has a legacy of spaceborne Ku-band scatterometers for ocean wind vector (both speed and direction) measurements. The Seasat Scatterometer was launched in 1978, and the NASA Scatterometer (NSCAT) was launched in 1996. Seasat had a single-sided swath, and NSCAT had a double-sided swath with variable incidence angles. However, the most important limitation with these scatterometers is that they only lasted for several months. The European Remote Sensing Satellite C-band Scatterometers (ERS-1 and ERS-2 Scatterometers) can measure long-term ocean wind vectors using a narrower single-sided swath; however, their resolution of 50 km for 4 to 8 revisited measurements per month is too coarse and too infrequent to be applicable to the Great Lakes.

On 19 June 1999, NASA launched the SeaWinds Scatterometer (denoted hereon as QSCAT) on the QuikSCAT satellite by a U.S. Air Force Titan II launcher. The launch of QSCAT marked the beginning of the first multi-year time-series (currently

going into the fifth year) dataset from a NASA Ku-band scatterometer. The sensor operates at Ku band (13.4 GHz), which can "see" through clouds and darkness. QSCAT measures backscatter ($\sigma_{0)}$, a quantity proportional to the ratio of received power over transmitted power, using a dual-beam rotating dish antenna. The antenna rotation makes conical scans of the Earth's surface with a swath of 1,800 km for the vertical polarization (V) on the outer beam and a swath of 1,400 km for the horizontal polarization (H) on the inner beam (Tsai *et al*. 2000). The larger swath covers 93% of the Earth in 1 day. Over the Great Lakes, QSCAT can provide a full coverage daily and as much as two times per day (~6 am and ~6 pm local time) over most of the lakes.

QSCAT has a very high relative radiometric accuracy of 0.2 dB, and the constant incidence angles of 46° (for H) and 54° (for V) enable simple and accurate measurements of wind speed and direction. QSCAT was designed to measure ocean wind vectors with the accuracy requirement of rms 2 m/s (3.9 knots) for the wind range of 3–20 m/s (5.8–38.9 knots) or 10% for the wind range of 20–30 m/s (38.9–58.3 knots), and rms 20° for wind directions over the wind range of 3–30 m/s (5.8–58.3 knots) (Jet Propulsion Laboratory 2001). These requirements are specified for a cell resolution of 25 km and no specification is listed for any higher resolution (Jet Propulsion Laboratory 2001).

Relationship of Wind Vector and Backscatter

After obtaining measurements of normalized radar backscattering cross section or backscatter (σ_0) the SeaWinds ground processing system uses these measurements to estimate wind vector fields. The relationship between wind and σ_0 has been extensively studied (Schroeder *et al*. 1982, Jones *et al*. 1982, Wentz *et al*. 1984, Li *et al*. 1989, Nghiem *et al*. 1997). The physical basis of this relationship is the fact that the microwave signal transmitted from the scatterometer interacts, mainly by the Bragg scattering mechanism, with wind-generated short-scale gravity-capillary waves, so that backscatter increases with increased wind speed (Plant 1986, Donelan and Pierson 1987, Phillips 1988, Quilfen *et al.* 1999). In particular for lake environments, a recent study in Lake Superior indicates that radar backscatter can be dominated by scattering from wind-driven capillary waves (Winstead *et al.* 2002).

The backscatter is sinusoidally modulated in azimuth by wind, and it peaks when the radar signal is transmitted perpendicular to the wave fronts and thus parallel to wind direction. There is a slight difference in the backscatter depending on whether the wind is blowing toward or away from the sensor; this is known as the upwind-downwind asymmetry. This relationship allows a unique wind vector (speed and direction) to be determined from noise–free σ_0 measurements provided that co-located and contemporaneous measurements are obtained from a combination of at least three different polarizations and look directions.

Because of the complexities in oceanic and atmospheric interactions at the interface (Plant 1986, Donelan and Pierson 1987, Phillips 1988, Nghiem *et al*. 1997), the development of a quantitative theoretical model has proven difficult. For this reason, empirical mappings from wind speed and direction to σ_0, in terms of a second harmonic function, have been developed using scatterometer data and in-situ wind measurements (Jones *et al*. 1982, Wentz and Smith 1999). Such mapping is known as a geophysical model function (GMF). To date, several versions of GMF have been obtained for near-surface wind retrieval over oceans. Although no GMF has been developed specifically for lake environments, we expect, to the first-order, a relationship between backscatter (σ_0), and lake wind vector to be similar to an ocean GMF. This is because major differences between lake and ocean environments are salinity and fetch, which weakly affect backscatter on a higher order (Donelan and Pierson 1987, Nghiem *et al*. 1995, Nghiem *et al*. 1997).

Standard Wind Processing

The SeaWinds ground processing (SGP) system makes use of an ocean GMF to estimate wind vector. Measured σ_0 is inverted for wind speed and direction using a maximum likelihood estimation approach. The result of this inversion is a set of four or fewer ambiguous solutions for wind vector (ambiguities) for each 25 km by 25 km grid location. Although QSCAT measurements satisfy the theoretical conditions for determining a unique wind vector for most of its swath wherever data from both beams are available, the presence of noise in each σ_0 measurement leads to ambiguous solutions. Ambiguous wind solutions have been reported for all spaceborne wind scatterometers employed to date. Information from neighboring grid cells or external wind fields are incorporated to reduce this ambiguity. Usually there are one or two ambiguities that are much more likely than the oth-

ers. Nonetheless, it is necessary to employ an ambiguity removal algorithm.

The ambiguity removal algorithm used by SGP has been optimized to limit the use of external wind information to cases in which the instrument's own directional discrimination is inherently poor (i.e., low wind speeds and single beam regions in the swath). An initial wind vector choice is made by a process known as thresholded nudging (Stiles *et al*. 2002). First, the choice is narrowed to vectors above a threshold likelihood value. Next, the closest of those vectors to a contemporaneous NCEP (National Centers for Environmental Prediction) 1° by 1° analysis field is chosen. A final unambiguous wind field is determined by performing multi-pass median filtering on the initialized wind field. During each pass, the median filter is applied to every grid cell in the field. For each grid cell, the ambiguity closest to the median of its surrounding 7 by 7 neighborhood is chosen.

Another important component of SGP is the direction interval retrieval algorithm (DIR) (Stiles *et al*. 2002). DIR was designed to improve directional accuracy of QSCAT wind vectors for sub-optimal viewing conditions. This is important because one such sub-optimal viewing condition is the reduction in measurements (increased noise) caused by binning the measurements on a finer grid. DIR is essential for obtaining accurate high-resolution wind fields such as those needed over the Great Lakes.

DIR is complementary to ambiguity removal. The latter addresses the problem of multiple peaks in the directional probability density function. DIR addresses the widening of those peaks under unfavorable conditions because of extra measurement noise or poor viewing geometry. DIR involves two modifications in wind retrieval. First, during maximum likelihood estimation (GMF inversion), a pair of directional error bars is computed for each ambiguous wind vector solution. These error bars are chosen so that the probability of the true direction being within the error bars of one of the ambiguities is 80%. Ambiguity removal is then performed in the usual manner. The second DIR modification is an additional median filtering step. Once final selected ambiguities have been chosen, median filtering is performed again to determine the best direction within the pair of error bars associated with the selected vectors. The error bars serve as hard limits restricting the amount of directional adjustment. DIR solution vectors obtained at the end of this process are stored in the QSCAT data product along with the selected ambiguities.

DIR makes use of spatial information to improve directional accuracy under unfavorable conditions. The use of spatial information from the surrounding neighbor pixels implies some degradation in resolution. However, regions with inherently good directional accuracy are not impacted. Such regions yield tight directional error bars around each ambiguity, and thus leave little room for change in the DIR processing. Even in cases where directional accuracy is initially poor, resolution degradation is mediated in several ways. First, only the resolution of directional information is impacted and high-resolution speed information is preserved. Second, the median filtering algorithm is an edge preserving method, so abrupt changes in direction along wide fronts are maintained. Only impulse-like changes in direction are lost in median filtering. In particular, tight spiral structures may be degraded. The same limitations are inherent in ambiguity removal itself. Complete details of the wind retrieval algorithm have been reported by Stiles *et al*. (2002).

High-Resolution Wind Processing

The wind retrieval methodology used to estimate high-resolution (12.5 km) wind fields over the Great Lakes differs from the standard approach in two important ways. First, QSCAT range-compressed measurements (called slice data) with a higher resolution of 7 km by 25 km are used rather than the full antenna footprint of 25 km by 35 km (called cell data). These high-resolution measurements are processed to obtain wind vectors on a 12.5-km wind field grid instead of the 25-km grid produced by standard processing.

Second, less strict land contamination flagging is applied so that any measurement with its centroid over water is included in the wind retrieval processing. Although the more lenient land flagging leads to noticeable land contamination in wind vectors near the shorelines, it is necessary because the conservative standard land flagging (50 km away from shore) only allows a limited number of wind vectors to be processed over the smaller lakes. On the other hand, a low-resolution wind result is affected when part of the 25 × 35-km footprint falls on land in near-coast areas. A difference when using high-resolution data is that the slice data may not fall on land while another fraction or part of the cell data may fall on land. Thus, the high-resolution data have a lesser impact due to land effects and can be used to obtain winds closer to land.

Slice data are noisier than the footprint measure-

ments and have a variable signal-to-noise ratio (SNR) depending upon where they are located in the antenna gain pattern. Binning them on a finer grid increases the effective measurement noise associated with each retrieved wind vector. Because of this increased noise, we report results for the DIR solution vectors only. DIR dramatically improves the accuracy of the directions in the high-resolution wind fields. It is especially important for the mid-swath vectors, which have a combined problem of poor viewing geometry and large (for high resolution) measurement noise.

The wind-vector product derived from QSCAT data has the advantage that it covers the Great Lakes region well spatially and often (as much as two times in every 24 hours) temporally. No other measurement provides this information over the extensive spatial extent of the Great Lakes on a daily basis. The increased resolution and more lenient land flagging are necessary modifications to achieve this result. The results are reasonably accurate as attested by comparisons with the GLCFS nowcast wind fields and with buoy data, despite limitations due to ocean GMF and near-shore contamination (to be addressed later in this paper).

GLCFS NOWCAST WIND FIELDS

The GLCFS run at NOAA GLERL produces nowcast wind fields over the Great Lakes, which can be used to compare with the satellite scatterometer results and to verify the wind vector measurements. We briefly review the method to calculate nowcast winds in this section.

In order to calculate heat and momentum flux fields over the water surface for the Great Lakes Forecasting System lake circulation model (Schwab and Bedford 1994), it is necessary to estimate wind and temperature fields at model grid points. The U.S. National Weather Service (NWS) and the Canadian Atmospheric Environment Service (AES) collect data from a network of various types of observation stations around the Great Lakes including Coast Guard stations, Coastal Marine Automated Network (CMAN) stations, National Data Buoy Center (NDBC) weather buoys, ships of opportunity, and airports as well as other stations close enough to the lakes to be considered "marine."

Observations from land stations, lake buoys, and ships form the basis for generating the needed gridded overlake wind and temperature fields. The use of wind data from land stations necessitates a correction due to differences in frictional effects between land and water, and another correction factor is applied to account for air-water temperature differences (Hubertz *et al*. 1991). The formulation to account for these correction factors was derived by Schwab and Morton (1984).

The initial implementation of GLCFS used either a distance-weighted or nearest neighbor algorithm to interpolate surface meteorological data to the computational grids for the nowcast part of the system. Subsequently, a new geometrically-based technique has been adopted. This technique appears to provide a more realistic representation of the two-dimensional wind field than previous techniques (Schwab *et al*. 1999). The approach is called "Natural Neighbor" interpolation and is based on the Delaunay triangulation of the station observation network as described by Sibson (1981) and by Watson (1994). The useful properties and advantageous characteristics of the method include:

1. The original function values are recovered exactly at the reference points,
2. The interpolation is entirely local (every point is only influenced by its natural neighbor nodes), and
3. The derivatives of the interpolated function are continuous everywhere except at the reference points.

According to Schwab *et al*. (1999), the first and second properties are especially important for the Great Lakes meteorological observation network, as not every station is available at every hour, and some stations (such as ships) appear only intermittently. Furthermore, this technique is also advantageous for interpolating data fields for which the spatial autocorrelation function is not well known, such as hourly wind fields.

COMPARISONS WITH GLCFS NOWCAST WIND FIELDS

Collocated and Contemporaneous QSCAT and GLCFS Nowcast Wind Fields

To demonstrate the capability of satellite scatterometry for daily large-scale measurements of lake wind fields, we compare QSCAT wind results with GLCFS nowcast wind fields. The QSCAT high-resolution wind processor produces wind vectors in zonal (u) and meridional (v) components in meters per second (m/s) for each wind vector cell in each orbit pass. The QSCAT wind speed is referenced to the height of 10 m, and it is the neutral

wind defined as the equivalent wind obtained with the stress and roughness length consistent with the atmospheric stratification when the stability adjustment is set to zero (Liu and Tang 1996). The GLCFS reports hourly nowcast wind direction in degrees and wind speed (also neutral wind at 10-m height) in knots. The nowcast wind field is interpolated over different grids with different grid density for different lakes: 15 km for Lake Superior and Lake Michigan, 10 km for Lake Ontario, and 5 km for Lake Huron and Lake Erie (the Lake Ontario grid was changed to 5 km on 14 October 2000).

To compare these results, we change QSCAT wind speed into knots (1 m/s = 1.9425 knots) and wind direction into degrees. This is because the GLCFS derived wind speeds are in knots and the final product for wind mapping is intended for distribution using standard operational units (e.g., knots for wind speed). We use the meteorological wind convention in which wind direction is defined as the direction from which the wind blows with respect to true North, clockwise, in degrees from 0 to 360.

The next step is to collocate QSCAT and nowcast wind in time and in space. First, we define a regular grid of 0.25° resolution in the geographic projection (0.25° in latitude and longitude). We bin QSCAT wind results into this grid for each orbit. Then, we select nowcast wind results closest in time (within half an hour) and bin them into the same grid. For each nowcast wind vector in a given pixel in the regular geographic grid, we select the QSCAT wind vector located at the closest distance. We require that the closest distance between QSCAT and nowcast data within the same lake to be less than 12 km. Furthermore, we eliminate any QSCAT wind result located within 25 km from shore to avoid QSCAT measurements that are strongly affected by land contamination, allowing a fair comparison between QSCAT and GLCFS nowcast wind results.

In the comparison of wind directions, we define the wind-direction difference as $\Delta\phi = \phi_Q - \phi_N$ where ϕ_Q is the QSCAT wind direction and ϕ_N is the nowcast wind direction. There is a wrap-around problem in the wind comparison. For example, if ϕ_Q = 359° and ϕ_N = 1° then $\Delta\phi$ = 358°. This value of $\Delta\phi$ is numerically large; however, there is actually only a 2° difference in the wind directions. In fact, the possible largest difference between the wind directions in the opposite direction of $\Delta\phi = \pm 180°$. To obtain a consistent comparison of wind directions, we wrap the result by adding or subtracting 360° to or from $\Delta\phi$ if $\Delta\phi$ is less than –180° or larger than +180°, respectively. Note that this operation is invariant because a wind direction does not change if it is turned around by ±360°.

We use the above approach to obtain collocated (in space) and contemporaneous (in time) QSCAT and nowcast wind-vector pairs to be compared. An advantage of this approach is that different grids, resolutions, and times of QSCAT and nowcast results can be accounted for with a single simple and effective computer code for all lakes. In the following sections, we present the comparison first for winds from light to moderate speeds, and then for a case of high winds before, during, and after a storm. These cases will demonstrate QSCAT's capability to measure winds over a wide range of surface conditions.

Light to Moderate Wind Range

During the time period from 1 to 20 October 2000, winds over the Great Lakes varied from very low winds (less than 4 knots) to moderately high winds (more than 32 knots). During this time, QSCAT completed 278 orbit revolutions from revolution number 6689 to 6966. Out of these orbits, 50 revolutions covered the Great Lakes. We derive wind vectors for each orbit swath over the lakes separately, and we do not combine data from different ascending and descending orbits to obtain the wind results.

Figure 1 presents scatter plots to compare collocated and contemporaneous QSCAT and GLCFS nowcast wind speed (upper panel) and wind direction (lower panel). We do not include winds below 4 knots because there is no requirement for QSCAT wind measurements in this low wind range. The continuous lines represent the linear regression, and the dashed lines are for the perfect fit. For all wind conditions over the Great Lakes during the 20-day period, QSCAT wind speed has a mean value of 15.1 knots with a standard deviation of 5.5 knots (representing the range of wind speed), while nowcast wind speed has a mean of 12.5 knots and a deviation of 4.3 knots. The linear regression analysis of QSCAT and nowcast wind speeds yields a regression coefficient of 0.920 (slope) with a small standard error of 0.005, and a regression constant (interception) of 3.65 knots with a standard error of 0.061 knots. The correlation coefficient between the wind speeds is 0.71. For all wind directions, the QSCAT mean value is 213° with a standard deviation of 109°, which compare well with 212° for the nowcast mean direction with a deviation of 101°.

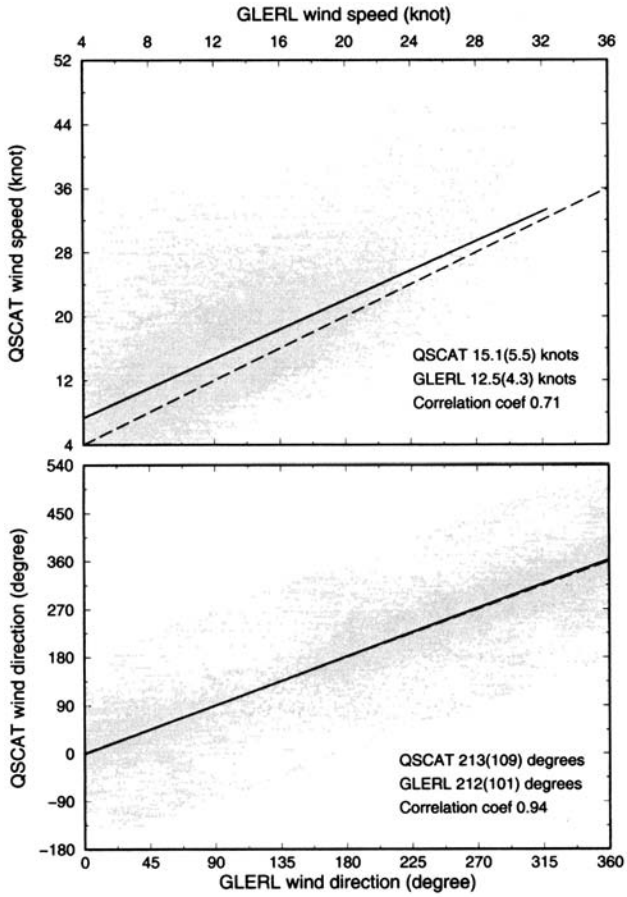

FIG. 1. Scatter plots of QSCAT and GLERL/GLCFS nowcast wind speeds and wind directions showing mean, standard deviation (in parentheses), and correlation coefficient.

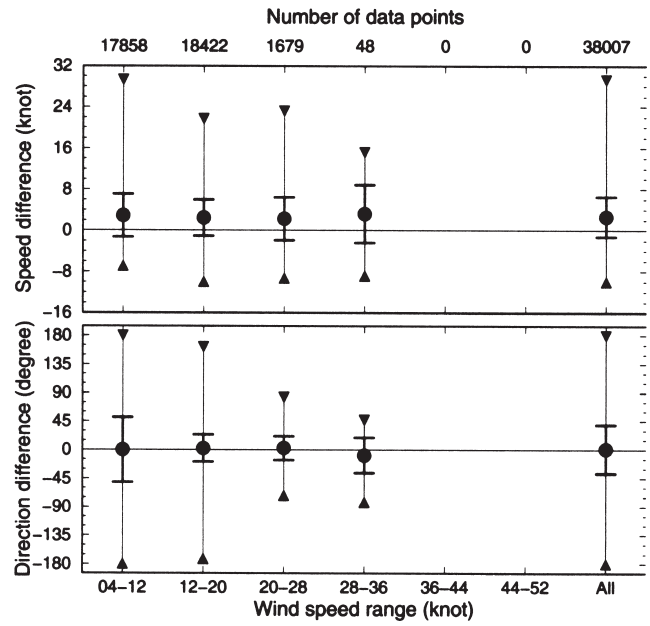

FIG. 2. Wind speed and wind direction differences between QSCAT and GLCFS results (QSCAT value–GLCFS value). Circles are for averaged values (bias between QSCAT and GLCFS), upper and lower bars for root-mean-squared deviations (rms error), and upper and lower triangles for maximum and minimum values (full range of difference).

The linear regression analysis shows an excellent fit between QSCAT and nowcast wind directions as indicated by a regression coefficient of 1.01 with a standard error of 0.002 and a regression constant of –0.7° with a standard error of 0.5°. The high value of 0.94 for the correlation coefficient confirms the excellent comparison of the wind directions.

Furthermore, we compare QSCAT and GLCFS results in terms of their differences in wind speeds and directions over different wind ranges as shown in Figure 2. The upper panel is for the comparison of wind speed, and the lower panel is for wind direction. The black circles represent averaged values, the upper and lower bars are for rms deviations (error bars), and the upper and lower triangles cover all values from maximum to minimum. The wind speed range is denoted along the lower horizontal axis, and the number of data points in each wind range is listed along the top horizontal axis in Figure 2. The upper panel in Figure 2 shows positive differences between QSCAT and nowcast wind speeds between 2.2 and 3.2 knots for different wind ranges, and an overall difference of 2.6 knots for all wind ranges from 4 to 36 knots. This result shows that there is a positive bias between QSCAT and GLCFS nowcast wind speeds (lower than the QSCAT values). The rms deviation ranges between 3.5 to 5.6 knots with the overall rms deviation of 3.8 knots for all of the wind ranges.

In order to evaluate the land contamination effects that may contribute to the bias in QSCAT wind speeds, we re-analyze the comparison between QSCAT and GLCFS winds by taking QSCAT data at least 50 km away from land. The results show very little change in the bias with a reduction of 0.4 knot (0.2 m/s) in the overall bias. However, the changes in bias are not uniform and can be larger for higher winds: 0.76 knot for the wind range of 20–28 knots, 0.29 knot for 12–20 knots, and 0.52 knot for 4–12 knots. Because (1) land effects should have a larger impact at lower winds

and (2) the change in the overall bias between 50-km and 25-km offshore wind speeds is small and well within the statistical uncertainty, it is likely that the bias over the various range of wind speeds is contributed to by other factors (e.g., effect of lake and ocean drag coefficients to be presented later), although land effects may remain important at low winds.

The lower panel in Figure 2 reveals an excellent comparison for wind directions with bias values between –8.8° and 2.4° for different ranges of wind speed. The overall average difference of 1.3° indicates that there is practically no bias in wind direction between QSCAT and GLCFS results. In terms of the rms deviation, the overall value for all of the wind ranges including low wind cases (4-12 knots consisting of 47% of all data used in Figures 1 and 2) is 38°. When we exclude the low winds, the rms deviation in wind direction significantly improves to 22°. This large reduction in the rms deviation indicates that high-resolution backscatter measurements (slice data) are too noisy to accurately retrieve wind direction at low winds.

With regards to the requirements for ocean wind measurements at the low resolution for which QSCAT is designed, the above results for lake wind speed (rms 3.8 knots) are quite consistent with the QSCAT requirement of rms 3.9 knots. This is remarkable given that: (1) we use an ocean GMF for lake environments, (2) we use high-resolution slice data, and (3) there are uncertainties in GLCFS nowcast winds. For wind directions, except at the low-wind range, the rms deviation of 22° is close to the QSCAT requirement of 20°. As a benchmark in assessing the performance of the QSCAT lake-wind measurements, we compare our results with a recently published evaluation of QSCAT ocean wind using buoy data (Ebuchi *et al.* 2002). QSCAT ocean winds in Level 2B (L2B) data have an rms deviation of 2 knots in wind speed and 23° in wind directions with respect to buoy measurements for winds from 6 to 46 knots (Ebuchi *et al.* 2002). Although the averaged speed bias for the ocean winds is small, the bias values are non-uniform and can be larger than +2 knots for low and high winds and negative for moderate winds (Ebuchi *et al.* 2002). Thus, except for the constant bias in lake wind speed (to be discussed in a later section), QSCAT performs well in measuring high-resolution wind vectors over the Great Lakes.

In Ebuchi *et al.*'s (2002) evaluation of QSCAT ocean winds, they selected only offshore buoys in deep water. Another factor affecting the comparison is due to shallow water and complex near-shore boundary conditions in addition to land-contamination effects. A comparison with buoys located at 100 km, 55 km, and 20 km offshore shows QSCAT low-resolution ocean wind measurements degrade quickly as the distance from shore becomes shorter, with the correlation coefficient decreasing from 0.89 to 0.56 and the rms error increasing from 4.3 knots to 7.8 knots in just the meridional wind component (Chao *et al*. 2003).

With the use of estimated wind directions, ocean wind results from ERS-1 SAR data, compared to buoy data, show biases ranging from 2.9 to 3.7 knots with rms deviation from 4.1 to 4.7 knots depending on different model functions (Fetterer *et al*. 1998). Note that ERS-1 SAR has small incidence angles (around 23°) where backscatter from the ocean surface is typically high; however, the small swath width (about 100 km) only covers a small section of the Great Lakes in any single orbit. RADARSAT-1 Scan SAR modes have a larger swath (400–500 km) which can cover a larger portion of the Great Lakes; however, the RADARSAT range of incidence angles is large and backscatter falls off precipitously at large incidence angles, especially for the horizontal polarization (Tsang *et al.* 1985) resulting in very noisy measurements. Compared to buoy measurements, RADARSAT ocean wind speed results have mean differences ranging from –3.1 knots to 4.1 knots with standard deviation from 4.5 knots to 6.0 knots for various fixed wind directions (Monaldo *et al*. 2001). Thus, SAR can be used to obtain wind speeds when a very high resolution (100 m) is required. If a frequent coverage over the large-scale Great Lakes and accuracy of wind vector measurements are necessary, a satellite scatterometer is a better choice.

A Storm with High Winds over the Great Lakes

We present wind vectors over all Great Lakes on 21, 22, and 24 October 1999 corresponding to conditions before, during, and after a storm with wind speed higher than 50 knots (according to QSCAT wind) and significant wave height larger than 20 feet. This high wind speed is classified in the wind range of 10 Beaufort (the strongest level is 12 for hurricane) on the Beaufort Wind Scale.

Figures 3, 4, and 5 (for 21, 22, and 24 October 1999) present the wind field mapping from QSCAT measurements together with the corresponding GLCFS nowcast results. QSCAT wind vectors are mapped over the Great Lakes using u and v compo-

nents in m/s over all wind vector cells in each orbit (the orbit revolution number is shown on top of each QSCAT wind map). QSCAT wind vectors are represented with arrows colored in a rainbow scale from blue to red for wind speeds from 10 to 40 knots (~5 to 20 m/s). In Figures 3, 4, and 5, GLERL nowcast wind fields are thinned and are presented on a 30-km grid for Lake Superior and Lake Michigan, and 20-km grid for the other lakes. These wind maps are for a general synoptic comparison of QSCAT and GLCFS winds; quantitative results are shown in Figure 6.

Before the storm (Fig. 3), the lake wind field measured by QSCAT shows light to moderate wind conditions in general agreement with nowcast results. During the storm (Fig. 4), QSCAT measurements reveal strong winds corresponding to the storm conditions. In this case, the QSCAT wind pattern indicates strong winds over central Lake Superior and central Lake Michigan. The QSCAT pattern also shows stronger winds over Lake Erie compared to those over Lake Huron and Lake Ontario. These QSCAT results are consistent with the corresponding nowcast wind fields during the storm. After the storm (Fig. 5), the wind subsided resulting in lower winds over Lake Superior and Lake Michigan compared to those on the other three lakes as observed in both QSCAT and nowcast wind fields. These results indicate that QSCAT has the capability to monitor storms over the Great Lakes.

To obtain a quantitative comparison between QSCAT and GLCFS nowcast results, we carry out an analysis similar to that presented in the previous section. Figure 6 consists of scatter plots for wind speed (upper panel) and wind direction (lower panel). Data points are plotted in blue, red, and green for the cases before, during, and after the storm, respectively. For the wind speed comparison, QSCAT results show 21.5 knots for mean wind speed with a standard deviation of 6.8 knots (for all QSCAT wind speeds) compared to 17.5 knots for the nowcast mean value with a deviation of 6.1 knots (for all GLCFS wind speeds). The regression coefficient for wind speed is 0.82, the regression constant is 7.2 knots, and the correlation coefficient is 0.73. For wind directions, QSCAT is in fair agreement with nowcast results as seen in the lower panel of Figure 6. The correlation coefficient for wind direction is 0.87, and the mean direction is 291° with a similar standard deviation for both QSCAT and nowcast results. The comparison over different ranges of wind speed is shown in Figure 7 for both wind speed difference (upper panel) and wind direction difference (lower panel). The overall average bias is 4.0 knots for wind speed (nowcast result is lower) with an rms deviation of 4.7 knots, and a negligible bias of –0.4° for wind direction with an rms deviation of 17°. Owing to the limited data in these three orbits, the analysis for the QSCAT and GLCFS wind vector comparison yields results not as statistically good as those from the 50 orbits for the case of light to moderate winds presented in the last section.

GLCFS nowcast wind fields are derived from measurements at stations on land together with data from CMAN stations and buoys in the lakes, and thus nowcast winds are expected to be consistent with these measurements at the station or buoy locations. As a simple check for both nowcast and QSCAT results during the storm, we extract data from the National Data Buoy Center (NDBC) for buoy 45004 located in Lake Superior at 47.65°N and 86.55°W (East Northeast of Hancock, Michigan, USA). This is a 3-m discus buoy where wind speed and direction are measured by an anemometer at 5-m height. Figure 8 presents the buoy wind speed (left panel) and significant wave height (right panel) measured in October 1999. At this buoy, the wind peaked at a maximum value of 37.7 knots on 23 October 1999 when the air temperature was 4.5°C and water temperature was 6.6°C. This is a slightly unstable condition with $z_0/L = -0.398$ (z_0 is the roughness scale, and L is the Monin-Obukhov length) and corresponds to a neutral wind speed of 40.9 knots at 10-m height derived from the formulation by Large and Pond (1981) for ocean momentum flux measurements. For the three cases corresponding to the conditions before, during, and after the storm in Figures 3, 4, and 5, Table 1 compares wind speed (translated to neutral wind at 10-m height) and wind direction results from buoy 45004, QSCAT, and GLCFS. Note that the GLCFS nowcast wind speed and direction results do not exactly match up with the buoy measurements because the grid-point location and the time of the nowcast operational product are not exactly the same as the location and time of the buoy data.

The above results for strong winds in the range of 36–44 knots (gale and strong gale force) show that QSCAT can measure wind speed with a bias of 2.1 knots and rms deviation of 4.5 knots, and wind direction with a bias of –10° and rms deviation of 22°. For winds around 42 knots, results for low-resolution ocean winds have a 6.4-knot bias and 7.8-knot rms deviation in wind speed, and 30° bias and

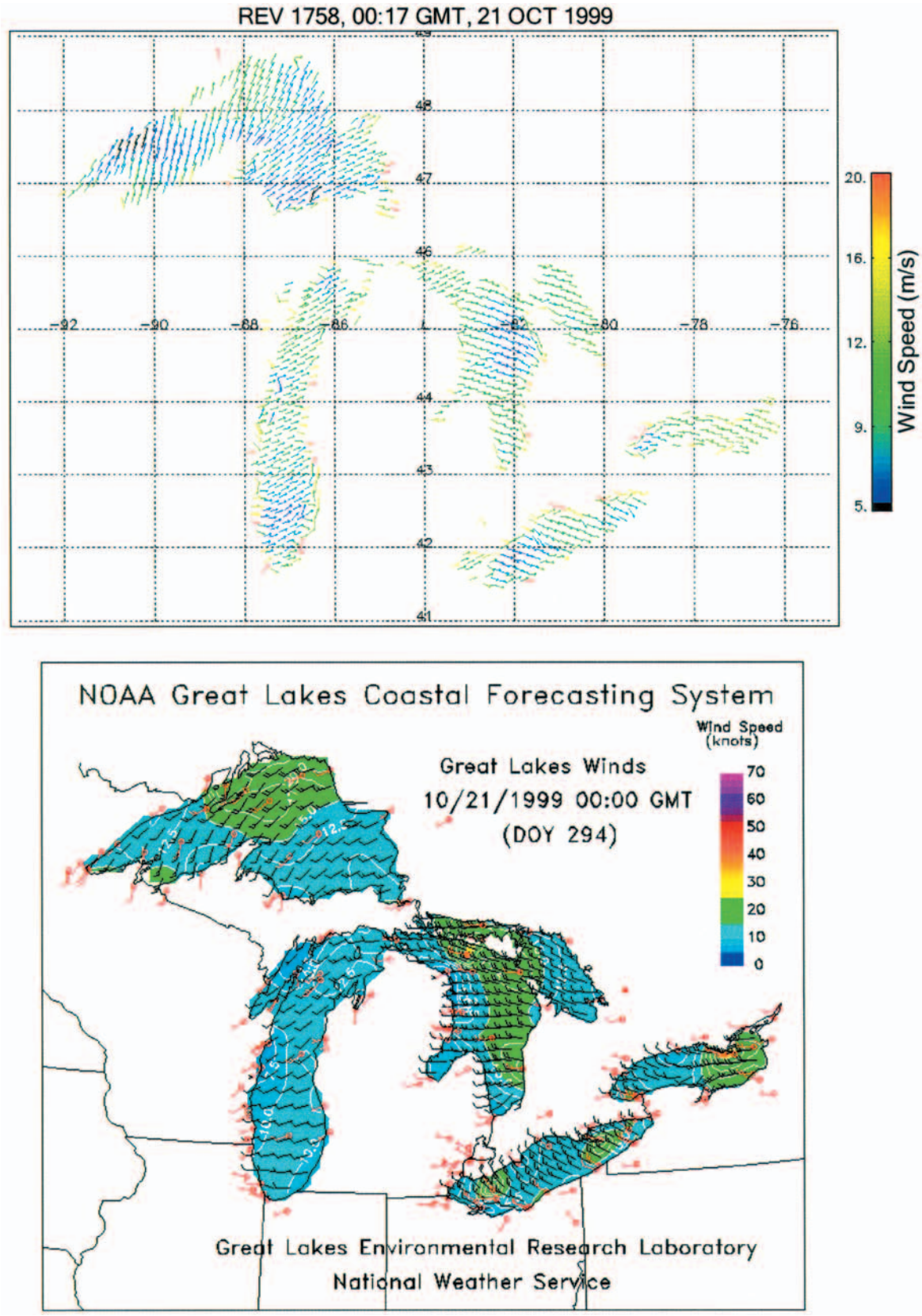

FIG. 3. Wind field over the Great Lakes on 21 October 1999 before the storm. The upper panel is for QSCAT vector wind results (standard output in m/s for wind speed), and the lower panel is for GLERL/GLCFS results (operational output in knots, 1 m/s = 1.9425 knots).

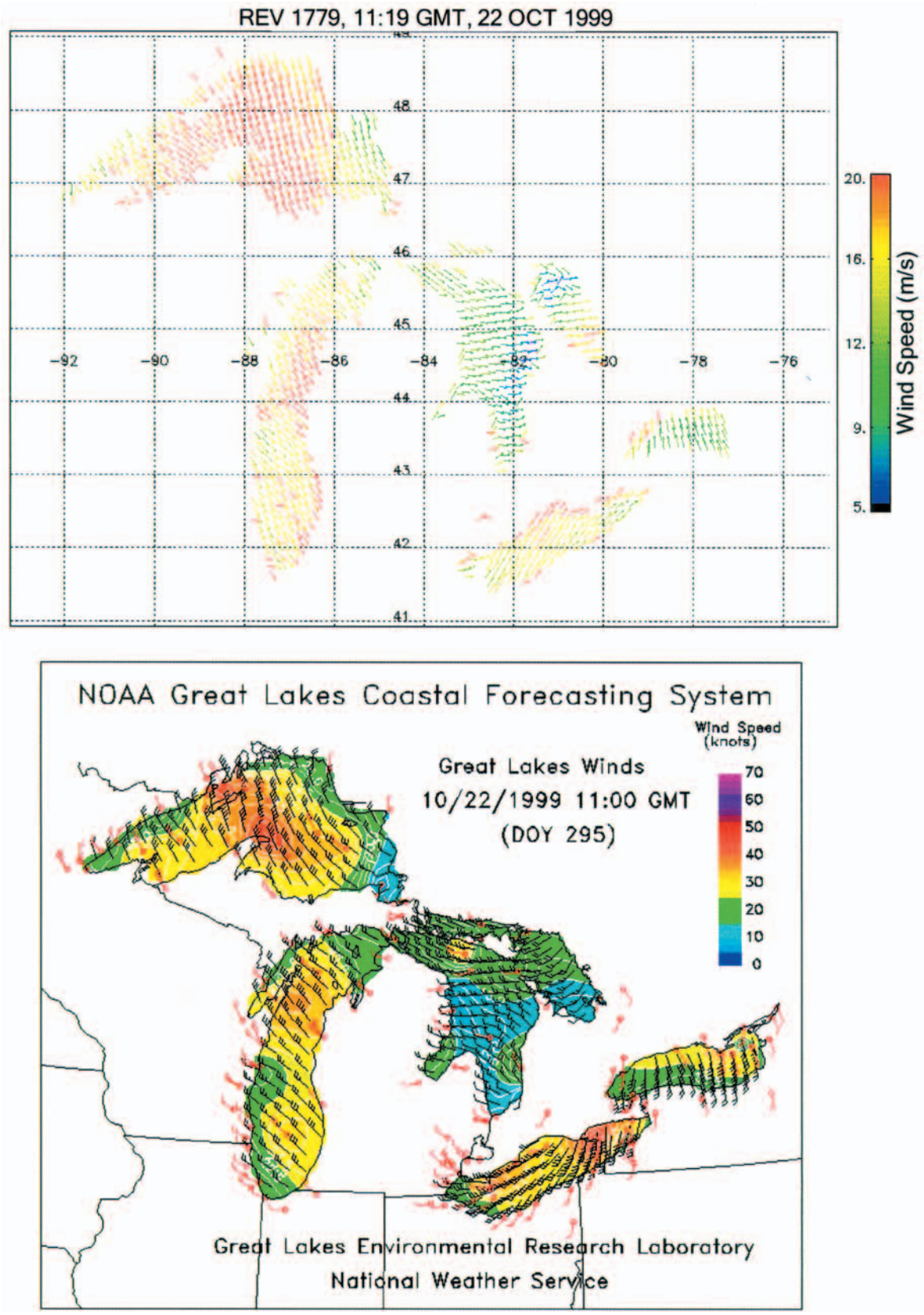

FIG. 4. Wind field over the Great Lakes on 22 October 1999 during the storm. The upper panel is for QSCAT vector wind results (standard output in m/s for wind speed), and the lower panel is for GLERL/GLCFS results (operational output in knots, 1 m/s = 1.9425 knots).

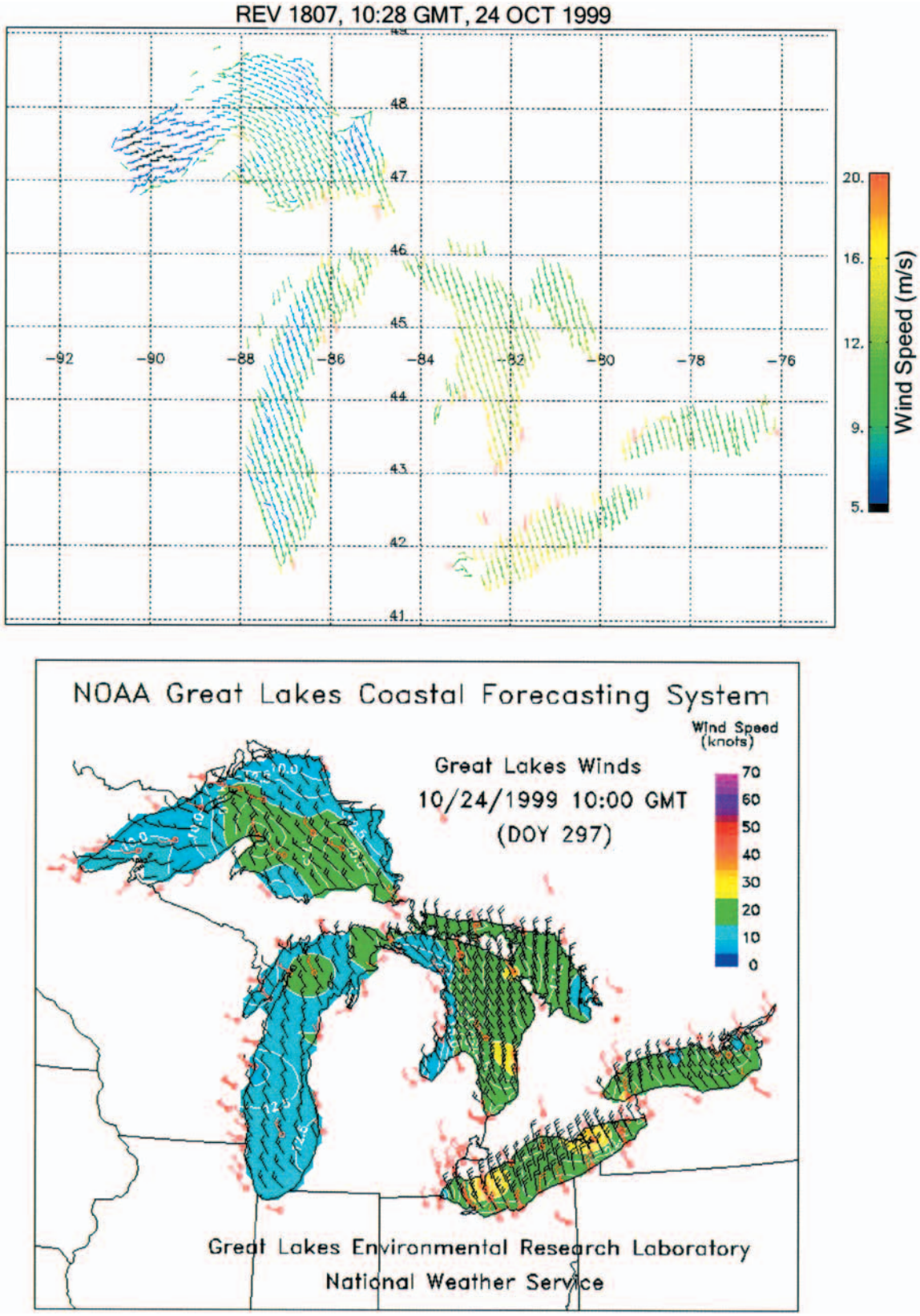

FIG. 5. Wind field over the Great Lakes on 24 October 1999 after the storm. The upper panel is for QSCAT vector wind results (standard output in m/s for wind speed), and the lower panel is for GLERL/GLCFS results (operational output in knots, 1 m/s = 1.9425 knots).

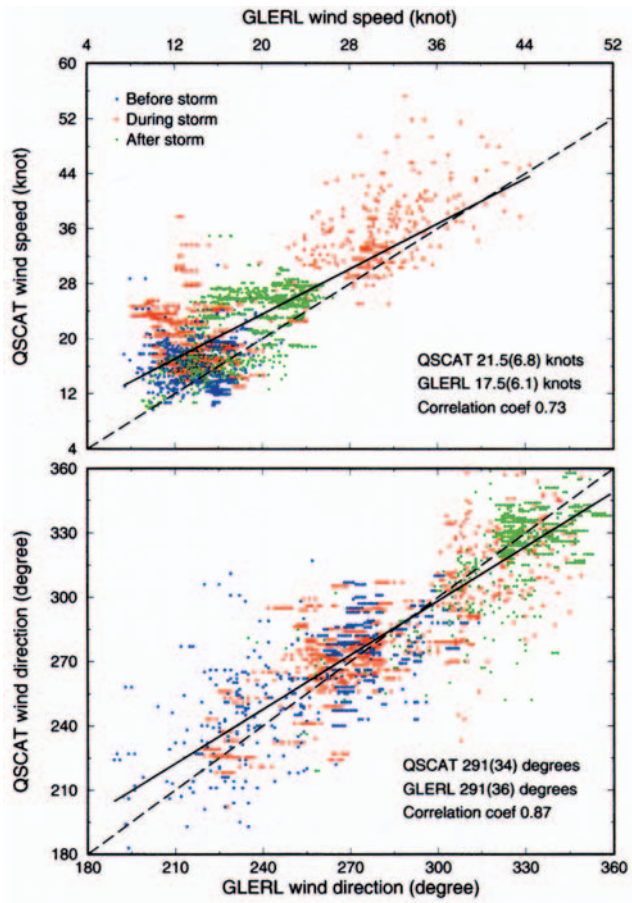

FIG. 6. Scatter plots of QSCAT and GLERL/GLCFS nowcast wind speeds and wind directions for cases before (blue dots), during (red dots), and after (green dots) a storm in October 1999.

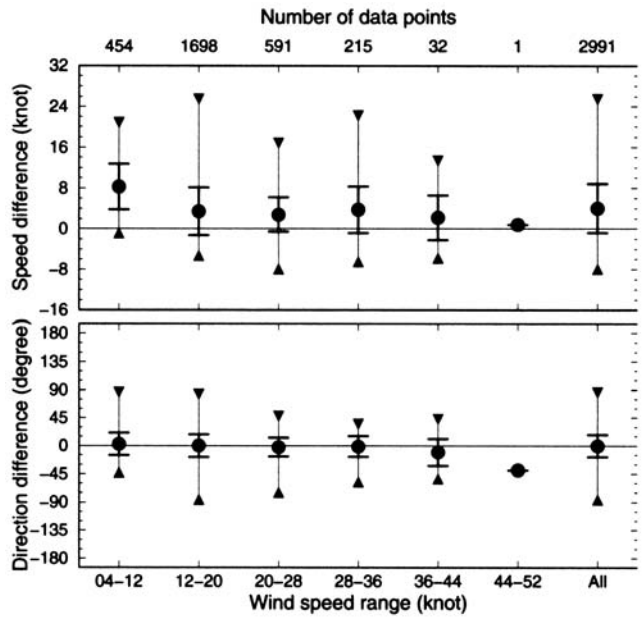

FIG. 7. Wind speed and wind direction differences between QSCAT and GLCFS nowcast results (QSCAT value–GLCFS value) over different wind ranges before, during, and after a storm in October 1999. Circles are for averaged values (bias between QSCAT and GLCFS), upper and lower bars for root-mean-squared deviations (rms error), and upper and lower triangles for maximum and minimum values (full range of difference).

14° rms deviation in wind direction (Ebuchi *et al.* 2002). Thus, for gales and strong gales, QSCAT performs relatively well in measuring high-resolution wind vectors over the Great Lakes. For all winds from gale force and stronger, 32-year wind statistics over the Great Lakes (MacLaren Plansearch Limited 1991) show only 3% in the range of 50–55 knots (strong gale to storm) and 1.7% stronger than 55 knots (violent storm to hurricane). Unlike over open ocean, hurricane-force winds occur extremely rarely over the Great Lakes. In a 1913 storm, one of the greatest to hit the Great Lakes, winds at 35–53 knots were recorded at the base of Lake Huron and 40–62 knots near Detroit. QSCAT backscatter is sensitive to winds up to 97 knots and the GMF is being improved for strong ocean wind measurements (Yueh *et al.* 2001). Nevertheless, a lake GMF needs to be developed such

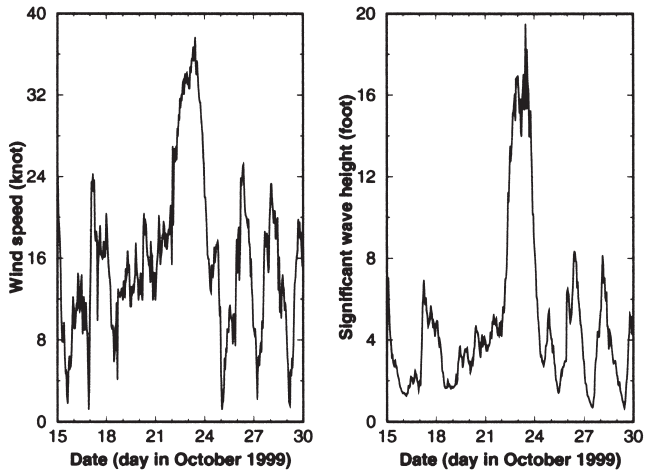

FIG. 8. Measurements by NDBC Buoy 45004 located in Lake Superior: (a) Left panel for wind speed at 5-m height, and (b) right panel for significant wave height.

TABLE. 1. Comparison of wind speed and wind direction results from buoy 45004, GLCFS, and QSCAT before (21 October), during (22 October), and after (24 October) a storm.

Date	Buoy	GLCFS	QSCAT
21 October 1999	15.5 kts, 235°	12.7 kts, 231°	14.6 kts, 237°
22 October 1999	34.5 kts, 323°	31.8 kts, 329°	36.3 kts, 330°
24 October 1999	16.4 kts, 299°	16.4 kts, 318°	15.5 kts, 324°

that it is useful for strong wind measurements over the Great Lakes. Good lake-wind measurements should include the range of 18–50 knots to be applicable to the NOAA National Weather Service (NWS) criteria for advisories and warning on the Great Lakes: 18–33 knots for small craft advisory, 34–47 knots for gale warning, and ≥48 knots for storm warning (National Weather Service 1999).

DISCUSSION

Satellite Wind Field Product

There are operational applications as well as scientific studies that require wind vector mapping over the Great Lakes. Near real-time wind information and short-term wind forecasts are important for commercial ship navigation and for U. S. Coast Guard icebreaking operations. Storm surges occur over the Great Lakes primarily due to extra-tropical cyclones or winter storms with high winds that can be intensified and cause severe and extensive damage (Danard *et al*. 2003). Thus, lake wind data are essential for hazard assessment and mitigation. The GLFS lake circulation model (Schwab and Bedford 1994) requires wind and temperature fields at model grid points to compute heat and momentum flux. The number of climate stations is not sufficient to provide long-term quality wind speed data to determine spatial lake effects to study Great Lakes impacts on regional climate (Scott and Huff 1996). Because of the wide range of applications of Great Lakes wind data, users from different agencies, organizations, and research institutes are expected. Potential users include the U.S. Coast Guard, the National Weather Service, the U.S. Army Corps of Engineers, shipping and fishing industries, universities, and national laboratories.

For operational purposes, we have produced a prototype product of wind field derived from QSCAT data over the Great Lakes as shown in Figure 9. Such a wind product can be developed and automated in the future for distribution to users on the Internet via web sites such as the Great Lakes CoastWatch node operated and maintained at GLERL, and then for archiving for future long-term scientific studies. In the wind product shown in Figure 9, colors represent the wind speed, and each full barb on the wind vectors denotes 10 knots. To show QSCAT results over all Great Lakes, we need to thin the actual wind array by a factor of 2 in the linear dimension or equivalently by a factor of 4 in two-dimensional space to avoid an overly dense number of wind barbs. A partition of the results in small regional sections for each lake can present the full-resolution wind-vector mapping in detail. For the particular example in Figure 9, all wind vectors were measured by a single sweep along orbit revolution number 1779 corresponding to the storm condition on 22 October 1999. With wide swaths, QSCAT can cover the Great Lakes up to two times per day. QSCAT has been acquiring global data including the Great Lakes continuously since 1999 and is going into the fifth year of data collection. Together with future scatterometers, the datasets can potentially provide long-term time-series of consistently calibrated wind fields over the Great Lakes.

Future Improvements

To improve the accuracy of QSCAT wind vectors over the Great Lakes, a GMF can be developed specifically for lake environments and better land contamination flagging can be applied. Currently, we use a GMF derived for ocean conditions to retrieve wind vectors over the fresh-water surface of the Great Lakes. Such a GMF may not be optimal for lake-wind applications, and an appropriate geophysical model function needs to be developed for lake surfaces. The land contamination problem can be addressed by either computing more accurate measurement boundaries in order to identify the measurements that are truly contaminated, or by developing a procedure to identify contaminated wind vectors after retrieval.

As seen in the above analysis, there is a bias between QSCAT wind speed based on the ocean GMF

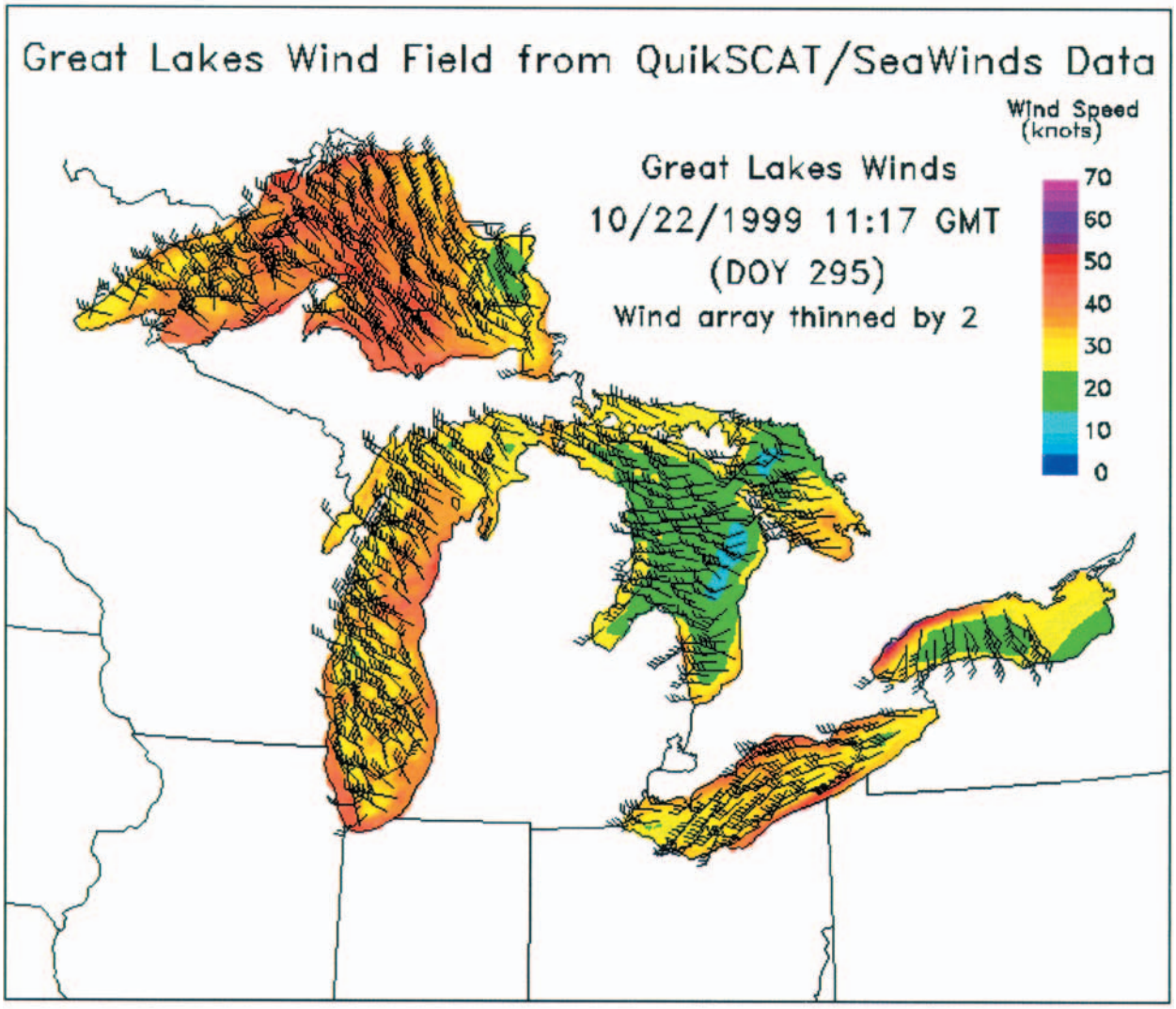

FIG. 9. Prototype of wind vector product for the Great Lakes derived from QSCAT data.

and GLCFS nowcast result based on marine observation data. One can tune the QSCAT result by empirically modifying the GMF (which is actually also an empirical function) to absorb the bias in the tuned GMF. This approach may reduce the differences, however, it does not provide a physical explanation for the wind speed bias. An approach presented by Colton *et al*. (1995) is to account for the difference in the drag coefficients between the lake and ocean environments. For the same friction velocity, lake neutral wind can be related to ocean neutral wind by the relationship (Colton *et al*. 1995):

$$U_{N_Lake}(10\text{m}) = [C_{DN_Sea} / C_{DN_Lake}]^{1/2}\, U_{N_Sea}(10\text{m})$$

where C_{DN_Lake} and C_{DN_Sea} are the drag coefficients, and $U_{N_Lake}(10\text{m})$ and $U_{N_Sea}(10\text{m})$ are the neutral wind speeds at 10-m height for lake and ocean, respectively. Colton *et al*. (1995) present expressions for lake drag coefficients for different finite values of fetch. They also report ocean drag coefficients over a range of stability conditions corresponding to different wave age and wave steepness associated with short fetch. Their results indicate that the drag coefficient on the lake has a steeper slope as a function of wind speed, and lake neutral wind speed is lower than that of the oceanic counterpart at the same friction velocity. This explains why an ocean GMF may overestimate lake winds causing a positive bias in the QSCAT results. However, the effect on the overall bias is complex

and is dependent on different values of fetch and wind speed distribution statistics over different lakes. Colton *et al*.'s relationship can be implemented in the QSCAT high-resolution lake-wind retrieval processor to translate ocean winds to lake winds to improve the QSCAT results. Nevertheless, direct measurements (both satellite and in situ surface data) over the Great Lakes should be used to develop a new GMF, specifically for lake environments including strong winds that can improve the accuracy of the wind retrieval from satellite scatterometer data. Long-term QSCAT data and the presence of a large amount of co-located in-situ observations should facilitate the development of a Great Lakes GMF.

A possible approach to improve Great Lakes wind mapping is that QSCAT wind fields obtained with a Great Lakes GMF are assimilated or blended, together with point measurements from land stations and lake buoys, into a regional-scale Great Lakes model, such as the GLCFS, to produce an optimized nowcast wind product. Because the current GLCFS can take input wind data at different location, time, and grid size, it is already suitable to ingest QSCAT winds into the nowcast model. There is a two-fold advantage to this approach: (1) effects of land contamination can be limited by weighting more on shore-station measurements, and (2) offshore wind measurements by the scatterometer can better represent wind fields over large lake areas, especially over open surface water during winter when buoys are retrieved and ship data are not available. Furthermore, the optimal wind fields can be used in the GLCFS for better wind forecast. The next generation of advanced satellite scatterometers should have a resolution between 4 and 10 km to measure more detailed patterns of wind fields over the Great Lakes while land-contamination effects can be significantly reduced.

Furthermore, rain and ice are factors that need to be accounted for in wind retrieval. A method for rain detection and flagging has been developed and applied to low-resolution ocean wind retrieval (Huddleston and Stiles 2000, Stiles and Yueh 2002). By examining co-locations of the Special Sensor Microwave Imager (SSM/I) rain-rate measurements with QSCAT data over open water surfaces, we find that rain rate greater than 2 mm/hour occurs in only 2% of QSCAT wind vector cells at 25-km resolution. Such rain rates can significantly impact QSCAT backscatter for ocean winds up to 20 knots (Stiles and Yueh 2002). A method for high-resolution rain detection needs to be developed for application to high-resolution lake-wind retrieval. For Great Lakes ice mapping, we have developed a scatterometer algorithm and verified the results using field observations and in-situ measurements along the U.S. Coast Guard icebreaker *Mackinaw* ship tracks during the Great Lakes Winter Experiment in 2003 (Nghiem and Leshkevich 2003). Thus, a comprehensive result will be a composite product that maps daily wind, rain, and ice information over the Great Lakes (depending on the season) throughout the year.

ACKNOWLEDGMENTS

The research carried out by the Jet Propulsion Laboratory (JPL), California Institute of Technology, was supported by the National Aeronautics and Space Administration. Partial funding for S.V. Nghiem was provided by JPL under the Lew Allen Award for Excellence. The research carried out by the Great Lakes Environmental Research Laboratory was supported by the National Oceanic and Atmospheric Administration. Technical discussions and comments from Dr. David Schwab (GLERL) on lake winds are acknowledged as is the technical assistance provided by Gregory A. Lang (GLERL). GLERL Contribution No. 1305.

REFERENCES

Angel, J.R. 1995. Large-scale storm damage on the U.S. shores of the Great Lakes. *J. Great Lakes Res*. 21:287–293.

Beal, R.C. 2000. Toward an international storm watch using wide swath SAR. *Johns Hopkins APL Technical Digest* 21(1):12–20.

Bedford, K.W. 1992. The physical effects of the Great-Lakes on tributaries and wetlands—A summary. *J. Great Lakes Res*. 18:571–589.

Chao, Y., Li, Z., Kindle, J.C., Paduan, J.D., and Chavez, F.P. 2003. A high-resolution surface vector wind product for coastal oceans: Blending satellite scatterometer measurements with regional mesoscale atmospheric model simulations. *Geophys. Res. Lett*. 30(1), art. No. 1013.

Colton, M.C., Plant, W.J., Keller W.C., and Geernaert, G.L. 1995. Tower-based measurements of normalized radar cross-section from Lake-Ontario—Evidence of wind stress dependence. *J. Geophys. Res*. 100(C5): 8791–8813.

Danard, M., Munro, A., and Murty, T. 2003. Storm surge hazard in Canada, *Natural Hazards* 28(2–3):407–431.

Davidson-Arnott, R.G.D., and Fisher, J.D. 1992. Spatial and temporal controls on overwash occurrence on a Great-Lakes barrier spit. *Can. J. Earth Sci*. 29(1):102–117.

Donelan, M.A., and Pierson, W.J. 1987. Radar scattering and equilibrium ranges in wind-generated waves with application to scatterometry. *J. Geophys. Res*. 92(C5): 4971–5029.

Eadie, B.J., Schwab, D.J., Leshkevich, G.A., Johengen, T.H., Assel, R.A., Hawley, N., Holland, R.E., Lansing, M.B., Lavrentyev, P., Miller, G.S., Morehead, N.R., Robbins, J.A., and Van Hoof, P.L. 1996. Development of Recurrent Coastal Plume in Lake Michigan Observed for First Time. *EOS (AGU Transactions)* American Geophysical Union, 77(35):337–338.

_____, Schwab, D.J., Johengen, T.H., Lavrentyev, P.J., Miller, G.S., Holland, R.E., Leshkevich, G.A., Lansing, M.B., Morehead, N.R., Robbins, J.A., Hawley, N., Edgington, D.N., Van Hoof. P.L. 2002. Particle transport, nutrient cycling, and algal community structure associated with a major winter-spring sediment resuspension event in southern Lake Michigan. *J. Great Lakes Res.* 28:324–337.

Ebuchi, N., Graber, H.C., and Caruso, M.J. 2002. Evaluation of wind vectors observed by QuikSCAT/SeaWinds using ocean buoy data. *J. Atmos. Ocean. Tech*. 19 (12):2049–2062.

Fetterer, F., Gineris, D., and Wackerman, C.C. 1998. Validating a scatterometer wind algorithm for ERS-1 SAR. *IEEE Trans. Geosci. Remote Sens*. 36(2):479–492.

Gabriel, A.O., Kreutzwiser, R.D., and Stewart, C.J. 1997. Great Lakes flood thresholds and impacts. *J. Great Lakes Res*. 23:286–296.

Horstmann, J., Koch, W., Lehner, S., and Tonboe, R. 2000. Wind retrieval over the ocean using synthetic aperture radar with C-band HH polarization. *IEEE Trans. Geosci. Remote Sens*. 38(5):2122–2131.

Hubertz, J.M., Driver, D.B., and Reinhard, R.D. 1991. Wind waves on the Great Lakes: A 32 year hindcast. *J. Coastal Res*. 7(4):945–967.

Huddleston, J.N., and Stiles, B.W. 2000. A multi-dimensional histogram rain flagging technique for SeaWinds on QuikSCAT. In *Proc. Int. Geosci. Remote Sens. Symp*., pp. 1232–1234.

Jet Propulsion Laboratory. 2001. *QuikSCAT science data product user's manual* (version 2.2). Jet Propulsion Laboratory Publ. D-18053, Pasadena, CA.

Jones, W.L., Schroeder, L.C., Boggs, D.H., Bracalente, E.M., Brown, R.A., Dome, G.J., Pierson, W.J., and Wentz, F.J. 1982. The SEASAT-A satellite scatterometer: the geophysical evaluation of remotely sensed wind vector over the ocean. *J. Geophys. Res*. 87(C5):3297–3317.

Khandekar, M.L., and Swail, V.R. 1995. Storm waves in Canadian waters—A major marine hazard. *Atmosphere-Ocean* 33(2):329–357.

Kreutzwiser, R.D., and Gabriel, A.O. 1992. Ontario Great-Lakes flood history. *J. Great Lakes Res*. 18:194–198.

Krieger, K.A., and Klarer, D.M. 1991. Zooplankton dynamics in a Great-Lakes coastal marsh. *J. Great Lakes Res*. 17:255–269.

Large, W.G., and Pond, S. 1981. Open ocean momentum flux measurements in moderate to strong wind. *J. Phys. Oceanogr*. 11:324–336.

Lawrence, P.L. 1995. Development of Great-Lakes shoreline management plans by Ontario Conservation Authorities. *Ocean and Coastal Management* 26(3):205–223.

Lesht, B.M., Stroud, J.R., McCormick, M.J., Fahnenstiel, G.L., Stein, M.L., Welty, L., and Leshkevich, G.A. 2002. An event-driven phytoplankton bloom in southern Lake Michigan observed by satellite. *Geophysical Research Letters*. 29(8):18-1–18-4.

Li, F.K., Large, W., Shaw, W., Walsh, E.J., and Davidson, K. 1989. Ocean radar backscatter relationship with near-surface winds: A case study during FASINEX. *J. Phys. Oceanogr*. 19(3):342–353.

Liu, W.T., and Tang, W. 1996. *Equivalent Neutral Wind*. JPL Publication 96-17, Pasadena, California: Jet Propulsion Laboratory, California Institute of Technology.

MacLaren Plansearch Limited. 1991. *Wind and wave climate atlas. Vol. III, The Great Lakes*. Halifax, Nova Scotia, Canada.

Martner, B.E., Rauber, R.M., Rasmussen, R.M., Prater, E.T., and Ramamurthy, M.K. 1992. Impacts of a destructive and well-observed cross-country winter storm. *Bull. Amer. Meteorol. Soc*. 73(2):169–172.

Miner, T., Sousounis, P.J., Wallman, J., and Mann, G. 2000. Hurricane Huron. *Bull. Amer. Meteorol. Soc. 81*(2):223–236.

Monaldo, F.M., Thompson, D.R., Beal, R.C., Pichel, W.G., and Clemente-Colon, P. 2001. Comparison of SAR-derived wind speed with model predictions and ocean buoy measurements. *IEEE Trans. Geosci. Remote Sens*. 39(12):2587–2600.

National Weather Service 1999. *A Mariner's Guide to Marine Weather Services—Great Lakes*. NOAA National Weather Service. NOAA PA 98053.

Nghiem, S.V., and Leshkevich, G.A. 2003. *Great Lakes ice mapping with satellite scatterometer data*. Jet Propulsion Laboratory Publ. D-26362, Pasadena, CA.

_____, Li, F.K., Lou, S.H., Neumann, G., McIntosh, R.E., Carson, S.C., Carswell, J.R., Walsh, E.J., Donelan, M.A., and Drennan, W.M. 1995. Observations of ocean radar backscatter at Ku and C bands in the presence of large waves during the Surface Wave Dynamics Experiment. *IEEE Trans. Geosci. Remote Sens.* 33(3):708–721.

_____, Li, F.K., and Neumann, G. 1997. The dependence of ocean backscatter at Ku-band on oceanic and atmospheric parameters. *IEEE Trans. Geosci. Rem. Sens. 35*(3):581–600.

Phillips, O.M. 1988. Radar returns from the sea surface _ Bragg scattering and breaking waves. *J. Phys. Oceanogr*. 18:1065–1074.

Portabella, M., Stoffelen, A., and Johannessen, J.A. 2002. Toward an optimal inversion method for synthetic aperture radar wind retrieval. *J. Geophys. Res.* 107(C8):1–13.

Quilfen, Y., Chapron, B., Bentamy, A., Gourrion, J., Elfouhaily, and T.M., and Vandemark, D. 1999. Global ERS 1 and 2 and NSCAT observations: Upwind crosswind and upwind downwind measurements. J. Geophys. Res. 104(C5):11459–11469.

Plant, W.J. 1986. A two-scale model of short wind-generated waves and scatterometry. *J. Geophys. Res.* 91(C9):10,735–10,749.

Schroeder, L.C., Boggs, D.H., Dome, G., Halberstam, I.M., Jones, W.L., Pierson, W.J., and Wentz, F.J. 1982. The relationship between wind vector and normalized radar cross section used to derive SEASAT-A satellite scatterometer winds. *J. Geophys. Res.* 87(C5):3318–3336.

Schwab, D.J. 1989. The use of analyzed wind fields from the Great Lakes marine observation network in wave and storm surge forecast models. *Preprint Volume of the 2nd International Workshop on Wave Hindcasting and Forecasting*, Environment Canada, Atmospheric Environment Service, Downsview, Ontario, pp. 257–266.

_____, and Bedford, K.W. 1994. Initial implementation of the Great Lakes forecasting system: A real-time system for predicting lake circulation and thermal structure. *Water Poll. Res. J. Canada* 29(2/3): 203–220.

_____, and Morton, J.A. 1984. Estimation of overlake wind speed from overland wind speed: A comparison of three methods. *J. Great Lakes Res.* 10:68–72.

_____, Lang, G.A., Bedford, K.W., and Chu, Y.F.P. 1999. Recent Developments in the Great Lakes Forecasting System (GLFS). In *Proceedings: American Meteorological Society Third Conference on Coastal Atmospheric and Oceanic Prediction and Processes*, 3–5 November, 1999, New Orleans, LA, pp. 201–206.

Scott, R.W., and Huff, F.A. 1996. Impacts of the Great Lakes on regional climate conditions. *J. Great Lakes Res.* 22:845–863.

Shabica, C., and Pranschke, F. 1994. Survey of littoral drift sand deposits along the Illinois and Indiana shores of Lake Michigan. *J. Great Lakes Res.* 20:61–72.

Sibson, R. 1981. A brief description of natural neighbor interpolation. In *Interpreting Multivariate Data*, ed. V. Barnett, pp. 21–23. New York: John Wiley & Sons.

Stiles, B.W., and Yueh, S.H. 2002. Impact of rain on spaceborne Ku-band wind scatterometer data, *IEEE Trans. Geosci. Remote Sens.* 40(9):1973–1983.

_____, Pollard, B.D., and Dunbar, R.S. 2002. Direction interval retrieval with thresholded nudging: A method for improving the accuracy of QuikSCAT winds. *IEEE Trans. Geosci. Remote Sens.* 40(1):79–89.

Tsai, W.-Y., Nghiem, S.V., Huddleston, J.N., Spencer, M.W., Stiles, B.W., and West, R.D. 2000. Polarimetric scatterometry: A promising technique for improving ocean surface wind measurements. *IEEE Trans. Geosci. Remote Sens.* 38(4):1903–1921.

Tsang, L., Kong, J.A., and Shin, R.T. 1985. *Theory of Microwave Remote Sensing*. New York: John Wiley and Sons.

Watson, D. 1994. *An Implementation of Natural Neighbor Interpolation*. Dave Watson Publisher, Claremont, Australia.

Wentz, F.J., and Smith, D.K. 1999. A model function for the ocean normalized cross section at 14 GHz derived from NSCAT observations. *J. Geophys. Res.* 104(C5):11499–11514.

_____, Peteherych, S., and Thomas, L.A. 1984. A model function for ocean radar cross sections at 14.6 GHz. *J. Geophys. Res.* 89(C3):3689–3704.

Winstead, N.S., Sikora, T.D., Thompson, D.R., Mourad, P.D. 2002. Direct influence of gravity waves on surface-layer stress during a cold air outbreak, as shown by synthetic aperture radar, *Monthly Weather Rev.* 130 (11):2764–2776.

Yueh, S.H., Stiles, B.W., Tsai, W.Y., Hu, H., and Liu W.T. 2001. QuikSCAT geophysical model function for tropical cyclones and application to hurricane Floyd, *IEEE Trans. Geosci. Remote Sens.* 39(12):2601–2612.

Submitted: 27 May 2003
Accepted: 17 December 2003
Editorial handling: Barry M. Lesht